1.0

4.5
5.0
5.6
6.3

2.8   2.5

3.2   2.2

3.6

1.1

4.0   2.0

1.8

1.25   1.4   1.6

MICROCOPY RESOLUTION TEST CHART

NATIONAL BUREAU OF STANDARDS-1963-A

TR 78078 *NU*

BR65871

LEVEL *II*

ROYAL AIRCRAFT ESTABLISHMENT

*

Technical Report 78078
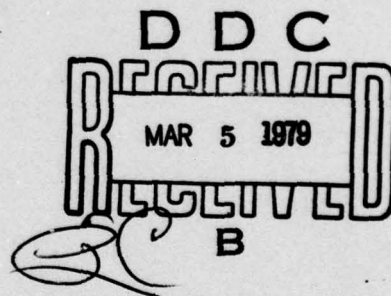
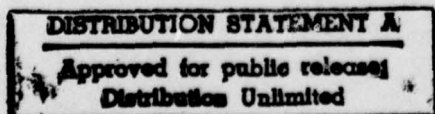July 1978

AN ANALYSIS OF A PROGRAMMED
LOAD FATIGUE FAILURE

by

C.J. Peel

D D C

RECEIVED

MAR 5 1979

B

*

Procurement Executive, Ministry of Defence

Farnborough, Hants

79 03 01 052

⑨ Technical reptis

⑱ DRIC

⑲ BR-65871

ROYAL AIRCRAFT ESTABLISHMENT

Technical Report 78078

Received for printing ⑪ 14 July 1978

⑥ AN ANALYSIS OF A PROGRAMMED LOAD FATIGUE FAILURE

by

⑭ RAE-TR-78078 ⑩ C. J. Peel ⑫ 29 p.

SUMMARY

Premature failure of an undercarriage fitting occurred during a fatigue test, in which the cylindrical barrel of the undercarriage was internally pressurised in a programmed sequence of pressures representing landing and taxying loads. Failure occurred by the initiation of fatigue cracks at defects in the undercarriage forging and by their growth to a critical depth. Measurement of the spacings of fatigue striations, on the surfaces of two cracks, enabled calculations to be made of the number of pressure sequences taken to grow the cracks from initiation to final failure.

An effective pressure range was calculated by comparison of the fatigue striation spacings with laboratory crack growth data. It was assumed that one cycle of the effective pressure range would produce the same rate of crack growth as an entire sequence of pressurisations. The effective pressure range was used to predict the fatigue life of a defect free undercarriage by reference to the pressure-fatigue life data found in the literature. It was found, by this means, that the metallurgical defects had reduced the life of the cylinder by a factor of at least 6 and that they had an effective stress concentration factor in fatigue of approximately 2.

Finally, the fatigue striation spacings were compared with rates of crack growth predicted from laboratory data by the addition of individual increments of crack growth caused by the individual pressure fluctuations. The predicted crack growth rate underestimated that observed by a factor of between 2 and 3 but this analysis revealed the damaging nature of small fluctuations, in pressure, about a high mean value.
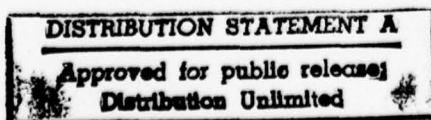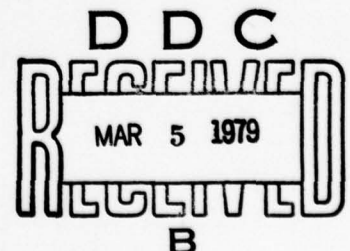
Departmental Reference: Mat 358

DDC
RECEIVED
MAR 5 1979
B

79 03 01 052

310 450

LIST OF CONTENTS

078

1 INTRODUCTION

The assessment of the airworthiness of an aircraft structure is based normally upon the results of full-scale laboratory fatigue testing of components of the aircraft. Ideally, these full-scale fatigue tests should duplicate the working environment of the aircraft. A correct simulation of the natural loadings and environmental conditions is, however, virtually impossible and usually the full-scale tests are simplified to the repeated application of a programme of loading cycles applied under laboratory conditions. The interpretation of the results of such tests is still complicated by the nature of the loading sequence, the complex geometry of the full-scale components and materials variables. This Report illustrates, in detail, a fractographic technique for the analysis of a typical full-scale test of an undercarriage fitting. The technique enables the effects of the programme of variable amplitude loads to be separated from those of defects in the forging and the introduction of the concept of an effective load, representing the entire sequence of variable amplitude loads, allows a fatigue life to be predicted for a defect-free forging. The fractographic technique relies upon the measurement, in the scanning electron microscope, of the spacings of fatigue crack striations that are formed on the fracture surface.

The use of the fatigue crack striation, in the quantitative analysis of fatigue failures, is now well established[1-3]. The basis of the method is that, in certain metals, increments of crack growth caused by the fluctuating fatigue stresses are individually marked upon the fracture surface by the formation of fatigue striations. The spacing of the striations is thus a measure of the local crack growth rate and counting the striations yields an estimate of the number of fatigue cycles involved in the growth of the crack between chosen limits of crack depth. Moreover, it has been demonstrated[2] that the crack growth rates, measured from striation spacings, can be compared with laboratory crack growth data to obtain the stresses causing the crack growth. This estimation is most conveniently accomplished with a fracture mechanics rationale.

2 FATIGUE TEST DETAILS

The undercarriage fitting (Fig 1) comprised a central hydraulic cylinder, pressurised by a sliding piston, and two large webs that ended in attachment lugs. The fitting had been machined from a forging of Al-Zn-Mg-Cu alloy to DTD 5104 specification and, in service, would be positioned vertically in the aircraft. Side loads and drag loads were applied by hydraulic jacks attached to the lugs on the webs and on the end of the cylinder.
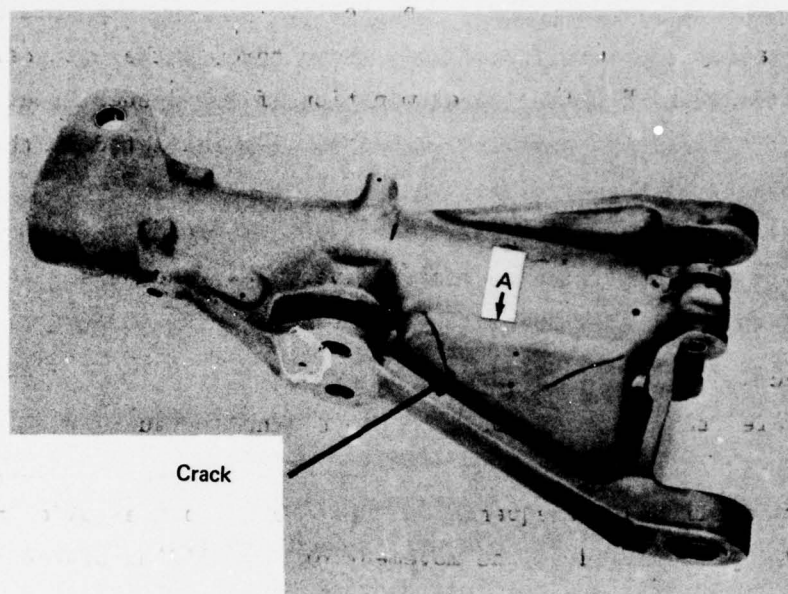
Fig 1   The undercarriage fitting after testing. The line of the
broken-through crack is indicated
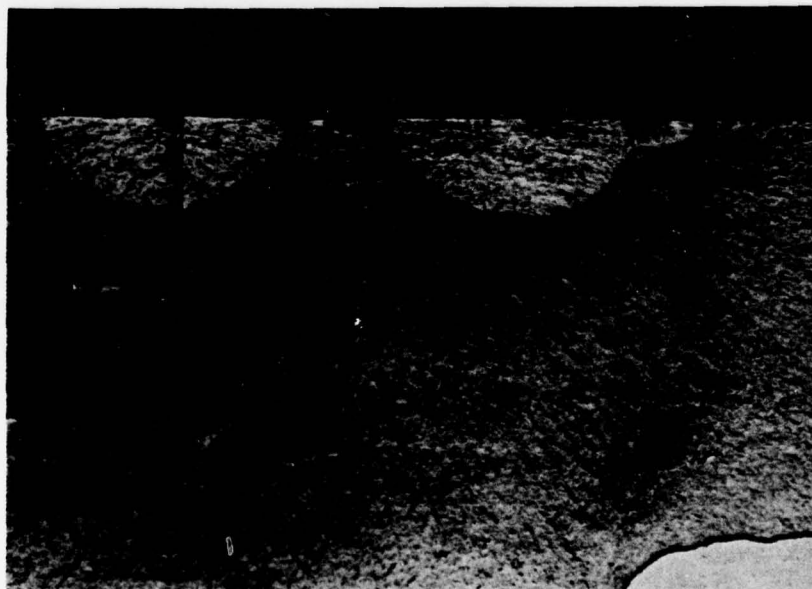
x2

Fig 2   Three fatigue cracks on the inner wall of the pressure
cylinder. Position A in Fig 1

TR 78078   C14970

The test was stopped, after the application of 2700 repeated programme sequences of loading, because a crack had grown through the cylinder wall and emerged in the web (see Fig 1). An examination of the opened fracture revealed three semi-circular fatigue cracks (Fig 2) that had initiated at the bore of the cylinder at position A (Fig 1). Two of these cracks had grown to critical depth of approximately 7 mm and subsequent cracking of the remainder of the cylinder and the web must have been rapid, requiring very few loading sequences, or even failing in one event.

An inspection of the loading sequences, applied to the undercarriage during the test, revealed that the stresses induced by the pressurisation of the cylinder would predominate in the formation and growth of the fatigue cracks. The side and drag loads were small and infrequent and are ignored in the following analysis. The cylinder was pressurised by the movement of its sliding piston and the end loads on this member were monitored and are shown (Fig 3) as the resulting pressure in the cylinder. The cylinder bore was approximately 116 mm in diameter.

One complete sequence of pressurisations consisted of one application of parts A and B (shown in Fig 3) followed by 11 applications of part B. The A and B parts of the first cycle are combined because the hydraulic pressure was maintained at the end of the A portion. The pressurisations simulate an air-ground cycle with taxying loads superimposed upon the high mean load as smaller load (or pressure) fluctuations.

3   FRACTOGRAPHY

Two fatigue cracks were examined at high magnifications. One of these cracks had grown in the region of the cylinder marked A in Fig 1 and the other, which was found subsequently, had grown in a similar manner further along the cylindrical barrel. (The position of this second crack is obscured in Fig 1.) It was apparent that both these fatigue cracks had initiated at defects in the forging. These defects were found to be similar in appearance and were 0.42 mm and 0.61 mm deep. The surface of one defect is illustrated in Fig 4. The oxidised appearance of the flaws suggested that they were casting defects that had not been closed by the forging process and that had been open to the surface during anodising and subsequently during the testing. The second of these defects was surrounded by a region of intergranular failure (Fig 5). The majority of the fracture surfaces of both cracks, however, was covered with conventional fatigue facets so the last 6 mm of cracking were the result of predominantly trans-crystalline fatigue failure, the crack depths at final failure being 7.6 mm and 7.0 mm. A closer examination of these fatigue facets revealed fatigue striations
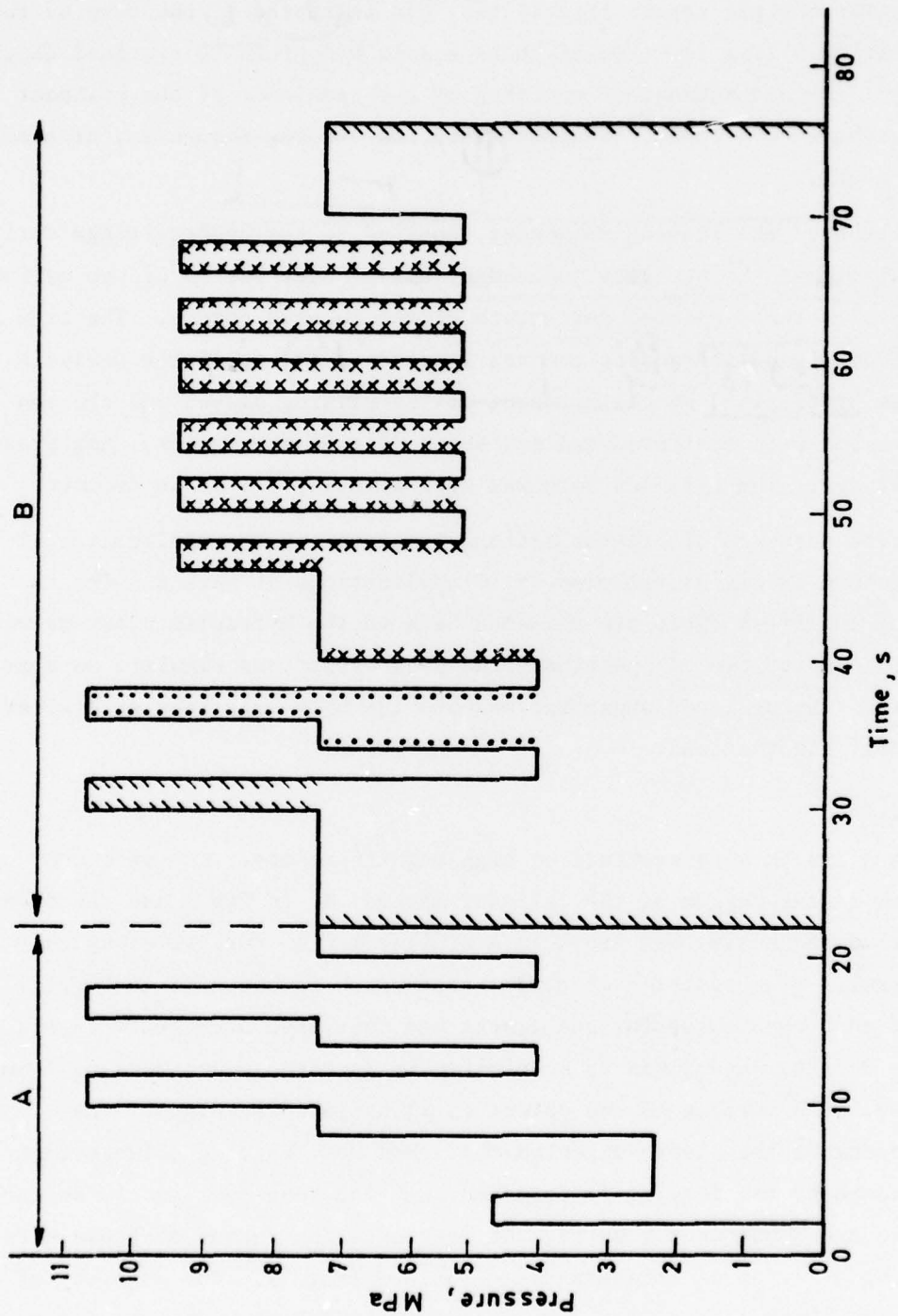
Fig 3

Fig 3   The A plus B pressure sequence. One complete fatigue programme consists of one
cycle of parts A + B followed by eleven cycles of part B. The B sequence is divided
into three parts for damage accumulation calculations. These are the air-ground
cycles (⊬), the large ground cycle (⁞) and six small ground cycles (l ₮)
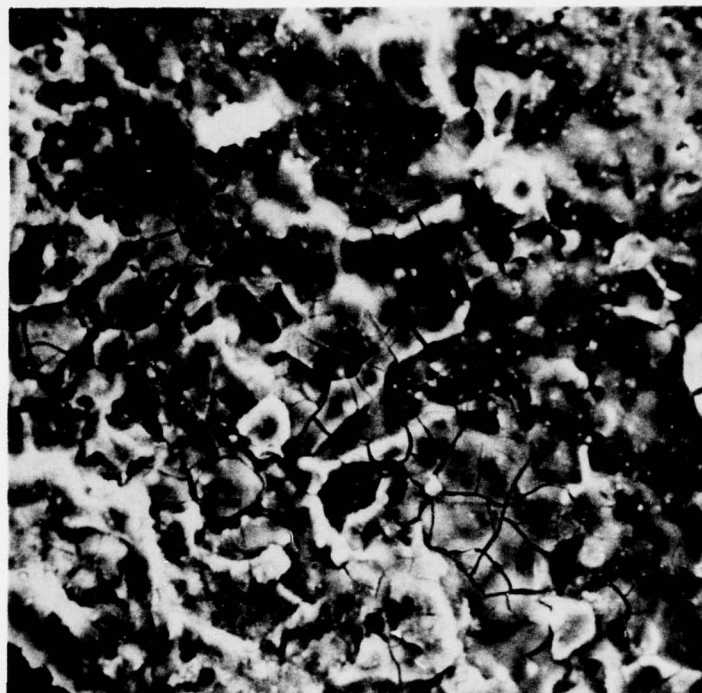
x300

Fig 4   The defect in crack 2
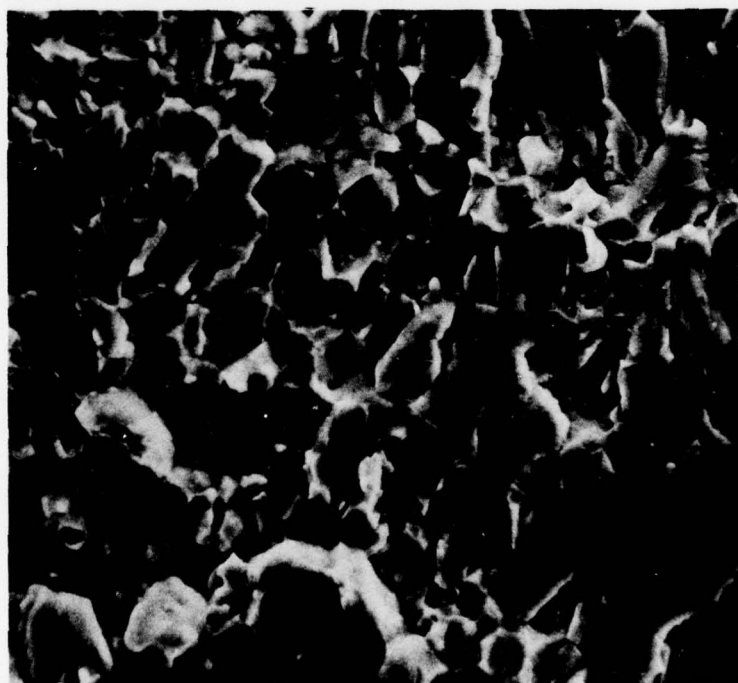
x800

Fig 5   Patches of intergranular cracking amidst fatigue facets
on the surface of crack 2

x7000

Fig 6 The fracture surface of crack 2 at a depth of **3.85 mm.**
Striations can be seen on the fatigue fracture facet
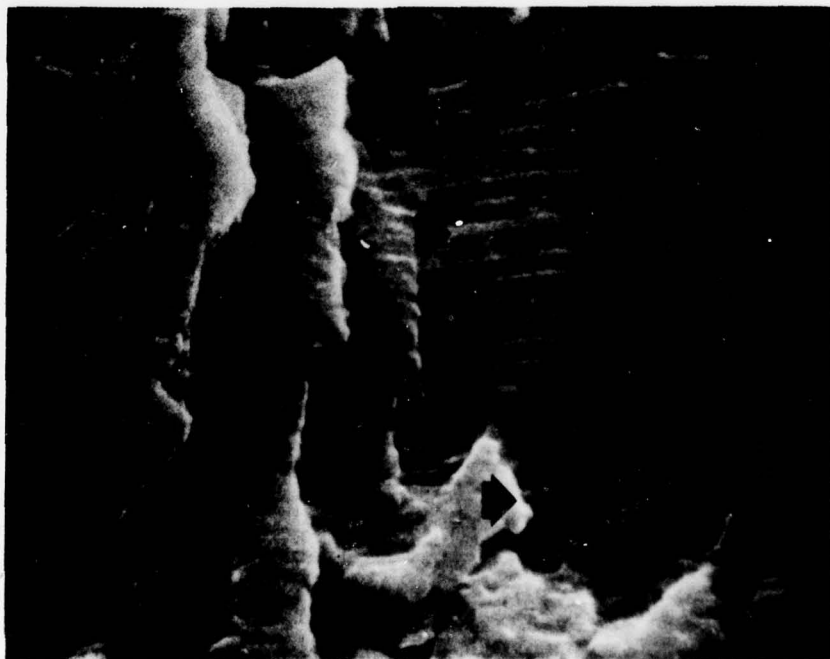
x4500

Fig 7 The fracture surface of crack 1 at a depth of **4.1 mm.**
The extra striation in the large A + B striation is arrowed

TR 78078   C14972

(Figs 6 and 7) with a distinct periodicity every twelfth striation, the inter-vening 11 striations being regularly spaced. These striations would thus seem to correspond to the $(A + B) + 11B$ sequence of loading (Fig 3), with the $A + B$ cycle appearing as a large striation. Thus these visible striations correspond to the variations in load between zero and a fluctuating maximum. An unsuccessful attempt was made to resolve detail within the striations corresponding to the smaller fluctuations in pressure about the high mean value. However, an extra marking could be resolved occasionally in the large $A + B$ striation (arrowed in Fig 7).

4   CRACK GROWTH RATE MEASUREMENT

The large $A + B$ striation was treated as a B sequence for the purposes of striation counting, that is all the striations in any one field of view were assumed to be identical. This must result in a slight over-estimate of the number of crack growth cycles. A logarithmic plot of crack growth rate $\frac{da}{dn}$, or striation spacing, was made as a function of crack depth 'a' (Fig 8). It appeared that crack 1 grew slightly faster than crack 2, although the difference in rate was hardly significant. Straight lines were fitted to the data for both cracks using regression analysis. Since the linear relation between $\log \frac{da}{dn}$ and $\log a$ was only approximately true, the best fit line was chosen as the bisector of the acute angle between the lines of regression of $\log \frac{da}{dn}$ upon $\log a$ and of $\log a$ upon $\log \frac{da}{dn}$.

5   CALCULATION OF THE NUMBER OF FATIGUE CRACK GROWTH CYCLES

The number $_iN^f$ of B pressure sequences taken to grow the two cracks from initiation at the defects, depth a_i, to final catastrophic failure, at crack depth a_f, was calculated. It was assumed that the crack growth rates $\frac{da}{dn}$ were a function of the crack depth a :-

$$\frac{da}{dn} = Ca^m \tag{1}$$

where C and m are constant with values readily determined from the plot of $\log \frac{da}{dn}$ versus $\log a$ (Fig 8). Equation (1) may be re-arranged and integration yields the value of $_iN^f$

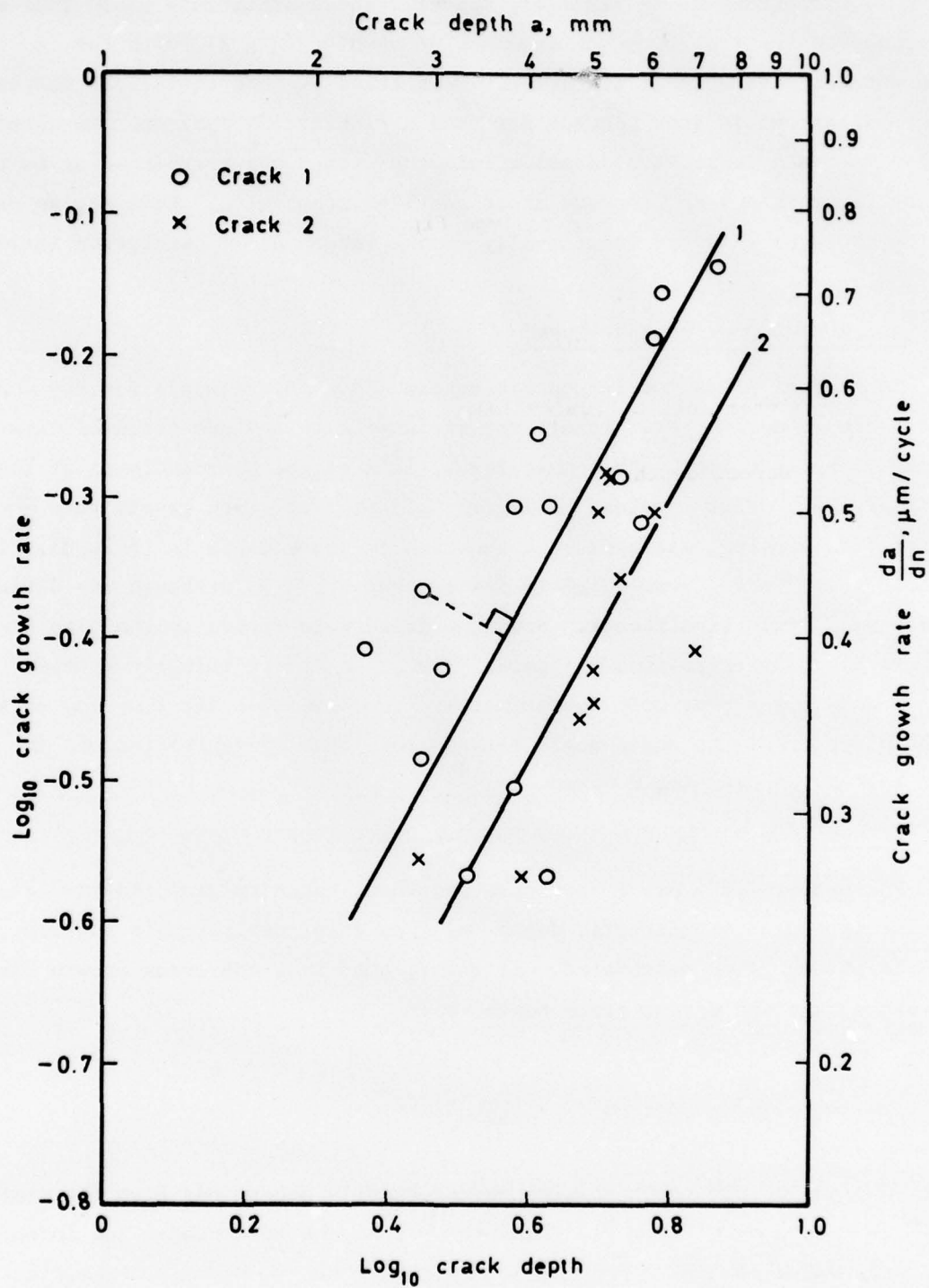$$_iN^f = \int_{a_i}^{a_f} C^{-1} a^{-m} da \tag{2}$$

Fig 8

Fig 8   Fatigue crack growth rates, measured as the spacing of striations
formed by the B pressure sequence

$${}_iN^f = C^{-1}\left[\frac{a^{1-m}}{1-m} + D\right]_{a_i}^{a_f}. \tag{3}$$

The number of complete pressure sequences $[(A + B) + 11B]$ is one twelfth of the number of B sequences ${}_iN^f$ calculated from equation (3). The results for the two cracks, and the relevant data from Fig 8, are:-

	Crack 1	Crack 2
Slope m $\left(\log\frac{da}{dn}\middle/\log a\right)$	0.91	0.92
Intercept C (μm/cycle)	0.124	0.091
Defect depth (mm)	0.42	0.61
Fracture depth (mm)	7.62	7.02
Number of B sequence crack growth cycles ${}_iN^f$	21380	28500
Number of programme sequences $[(A + B) + 11B]$	1780	2375

It would seem that the growth of the cracks from the defects to final catastrophic failure required at least 67% of the 2700 programme load sequences $[(A + B) + 11B]$ that were applied. It might be anticipated[4] that the initiation of fatigue cracks at the smooth bore of the cylinder, a plain fatigue situation, would require at least 80% of the total fatigue life leaving only 20% for crack growth. The fact that the cracks were growing for at least 67% of the fatigue life is thus an indication of the severity of the flaws in precipitately initiating the cracks. Moreover the measured life of 2700 cycles must have been reduced by the presence of these metallurgical defects. The estimation of a fatigue life for a defect free component was required, but was complicated by the programmed loading. However, an estimation of the fatigue life of a cylinder, free of defects, was made by determining an effective pressure range equivalent, in its effects upon crack growth rates, to the whole B cycle of pressures. The fatigue life of the cylinder could then be found from conventional stress (or pressure) - fatigue life data using this effective pressure.

6   CALCULATION OF THE EFFECTIVE PRESSURE RANGE Δp_e

The fatigue crack growth rates of the two cracks in the cylinder have been measured at increasing crack depths. If these crack growth rates are compared with rates measured[5] in the laboratory under uniform fatigue loadings as a function of the stress intensity factor range (ΔK), then ΔK can be determined as a function of crack depth in the cylinder. Since ΔK is a function of the pressure range inside the cylinder and the crack depth, the effective pressure range may be calculated. Here, the effective pressure range Δp_e is defined as the pressure range that, when applied in a repetitive manner to the cylinder, would have produced the same crack growth rates as those measured for the whole B loading sequence.

Pearson has provided[5] the necessary plots (Fig 9) of fatigue crack growth rates as a function of stress intensity factor range (ΔK) and for three different ratios of $\dfrac{\text{minimum stress intensity factor}}{\text{maximum stress intensity factor}}$.

The data most appropriate to the present case was for DTD 5050, an alloy of reasonably similar composition to DTD 5104, stressed transversely with a ratio of $\dfrac{\text{minimum stress intensity factor}}{\text{maximum stress intensity factor}}$ of 0.05 (Fig 9). Thus it is assumed that the whole of the B cycle acts as a single pressure cycle with $\dfrac{p_{min}}{p_{max}}$ equal to 0.05. Values of ΔK, read from Fig 9, are tabulated (Table 1) for increasing crack depths.

Solutions for the stress intensity factor for a radial crack in a long tube are available[6] in terms of pressure and crack depth and those of Bowie and Freese[7] are reproduced in Fig 10. These solutions are appropriate to a long cylinder, uniformly pressurised to p, and containing a radial crack which is open to the cylinder and is thus also pressurised to the value p. The stress intensity factor K_1 is given by:-

$$K_1 = \frac{K_1}{K_0} \frac{2pR_2^2\sqrt{\pi a}}{(R_2^2 - R_1^2)\phi} \tag{4}$$

where $\dfrac{K_1}{K_0}$ is a correction factor plotted in Fig 10 as a function of the crack depth and the ratio $\dfrac{R_1}{R_2}$ of the internal radius (R_1) to the external radius (R_2) of the cylinder. ϕ, a correction for crack front curvature was assumed to be constant at 1.4 for all crack depths.

Fig 9
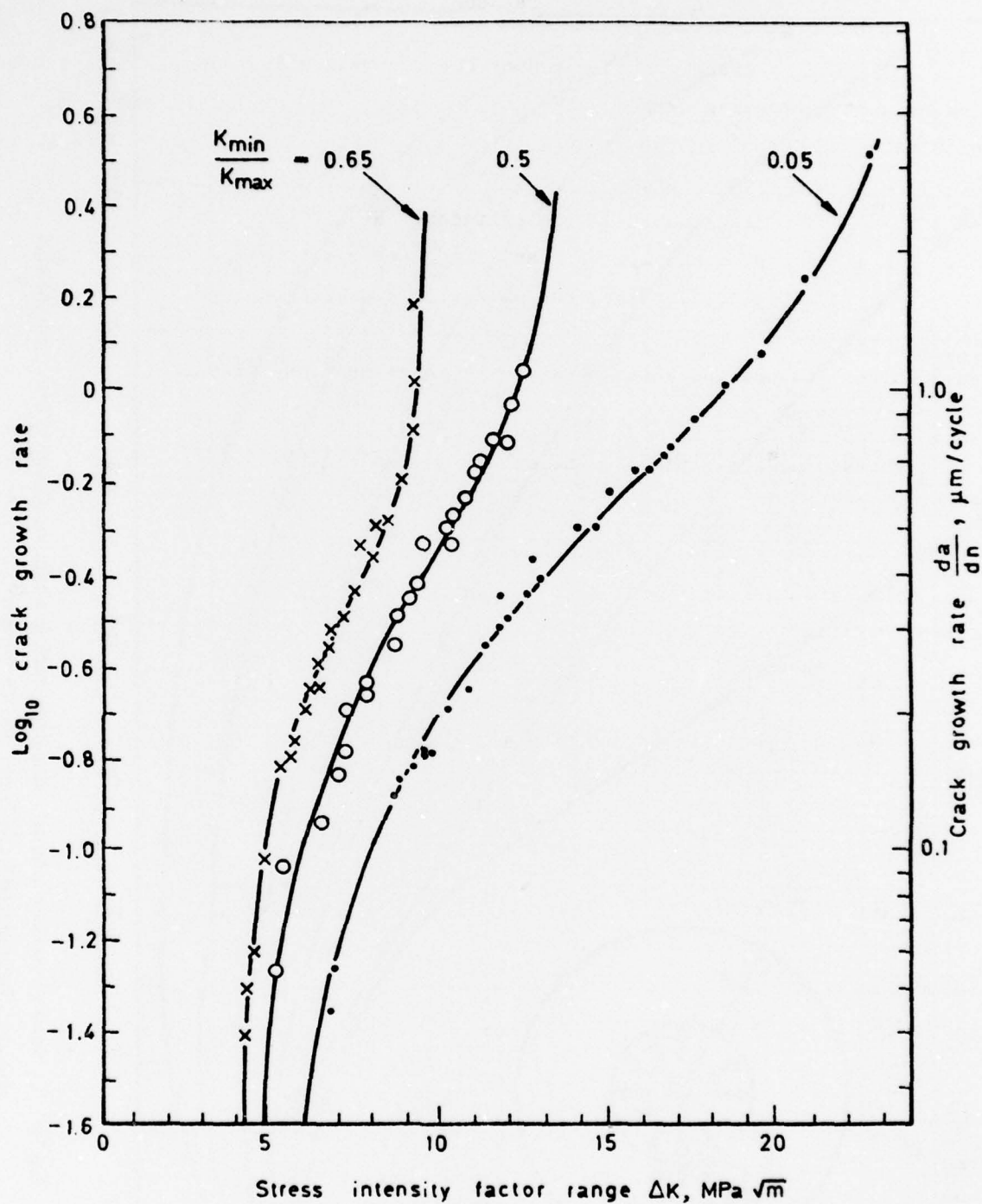
Fig 9   Fatigue crack growth rates, measured as a function of stress intensity factor range ΔK_1, for DTD 5050 alloy stressed at three ratios of $\dfrac{\text{minimum } K_1}{\text{maximum } K_1}$. Data from Pearson[5]
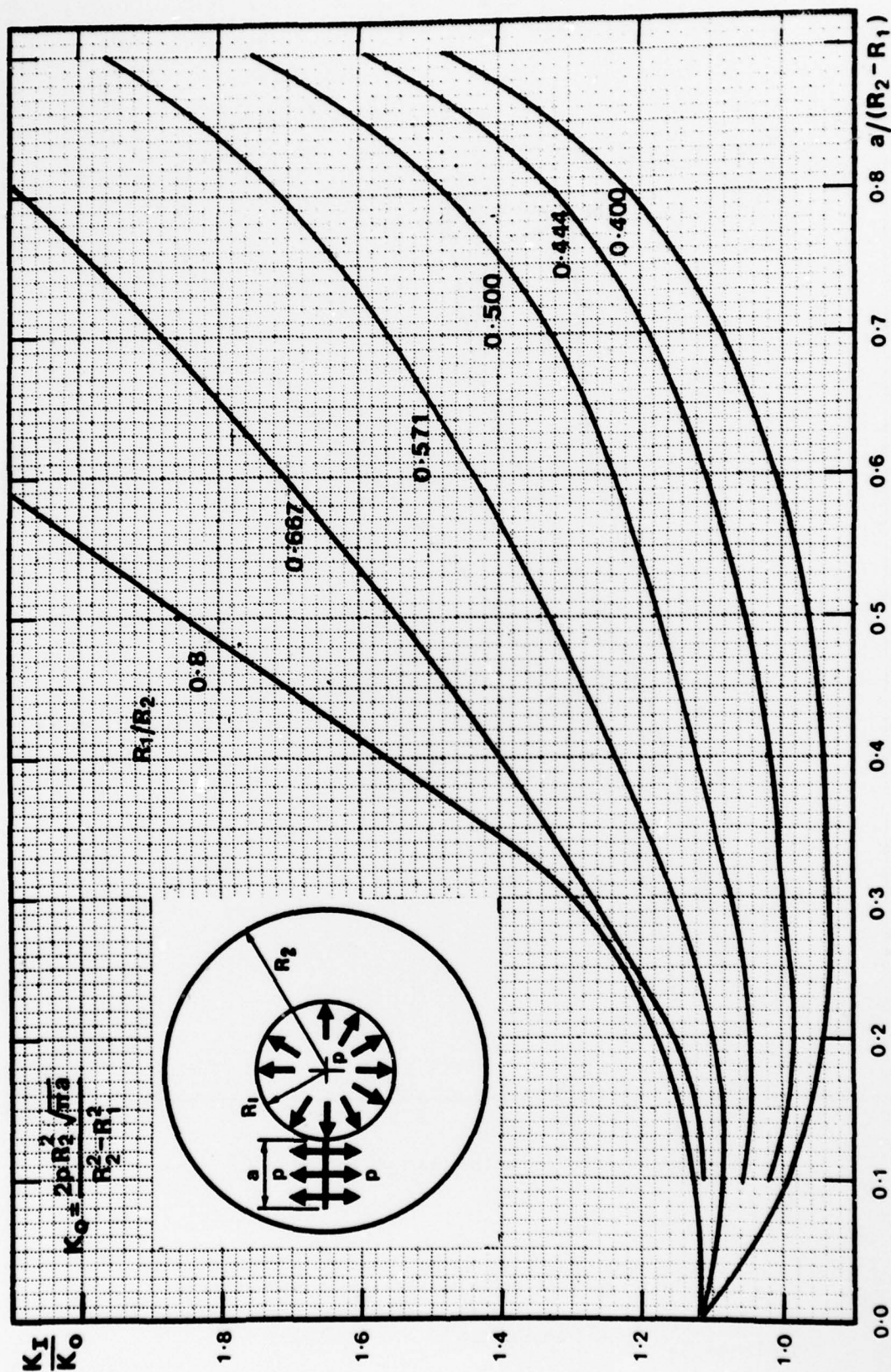
Fig 10

Fig 10 K_1 for a pressurised internal radial edge crack in a tube subjected to a uniform internal pressure.   Reproduced from Rooke and Cartwright[6]

Since the values of R_1 and R_2 for the examined cylinder were respectively 57.9 mm and 72.3 mm, the $\frac{K_1}{K_0}$ curve for $\frac{R_1}{R_2} = 0.8$, would seem to be most appropriate and values of $\frac{K_1}{K_0}$ were read from Fig 10 for each value of crack depth 'a' at which striation measurements had been made. A plot (Fig 11) was made of $\log_{10}\Delta K_1$, obtained from the striation spacing and Pearson data, versus $\log_{10}\frac{\Delta K_1}{\Delta K_0}\sqrt{\pi a}$, calculated from the $\frac{K_1}{K_0}$ values from Fig 10. It can be seen from equation (4) that:-

$$\log_{10}\Delta K_1 = \log_{10}\frac{\Delta K_1}{\Delta K_0}\sqrt{\pi a} + \log_{10}\frac{2\Delta p R_2^2}{\left(R_2^2 - R_1^2\right)\phi} \qquad (5)$$

where values of the *range* in stress intensity ΔK_1 and the *range* in effective pressure Δp_e are now considered. The data should fit a straight line with a slope of unity but a slope of only 0.4 was obtained (Fig 11). It is thus apparent that the web on the cylinder (see insert Fig 12) prevented the stress intensity factor from rising as predicted in Fig 10. A solution to this problem was compiled by assuming arbitrarily that, when small *ie* less than 2 mm deep, the crack would behave as if it were in a thin walled cylinder with $\frac{R_1}{R_2} = 0.8$ and that at depths greater than 6 mm the crack would behave as if it were in a thick walled cylinder with $\frac{R_1}{R_2} = 0.4$. These two solutions are combined (in Fig 12) with a smooth transitional region between crack depths of 2 mm to 6 mm.

$\log_{10}\Delta K_1$ versus $\log_{10}\frac{\Delta K_1}{\Delta K_0}\sqrt{\pi a}$ was replotted (Fig 13) using these new $\frac{\Delta K_1}{\Delta K_0}$ values and the desired slope of unity was obtained, moreover the scatter of the data about the lines for the two cracks was clearly reduced. The value of the term $\log_{10}\frac{2\Delta p R_2^2}{\left(R_2^2 - R_1^2\right)\phi}$ was readily obtained for each crack from Fig 13 and the effective pressure ranges Δp_e were calculated:-

Crack 1 $\Delta p_e = 27.3$ MPa

Crack 2 $\Delta p_e = 24.8$ MPa .

Thus an average value of the effective pressure range, that was assumed to be equivalent in its effects upon crack growth rate to the whole B sequence, was found to be 26 MPa.

Fig 11

Fig 11   Plot of log ΔK_1, from striation spacing and Pearson data[5], versus
calculated values of $\log \dfrac{\Delta K_1}{\Delta K_0} \sqrt{\pi a}$ with $\dfrac{\Delta K_1}{\Delta K_0}$ values taken from
the curve for $\dfrac{R_1}{R_2}$ = 0.8 in Fig 10

Fig 12

17

R_1 = 57.9 mm

R_2 = 72.3 mm

R_2' = 144.8 mm

$\frac{R_1}{R_2}$ = 0.8

Combined curve for undercarriage

$\frac{R_1}{R_2'}$ = 0.4

Crack depth a, mm

Normalised stress intensity factor, $\frac{K_1}{K_0}$
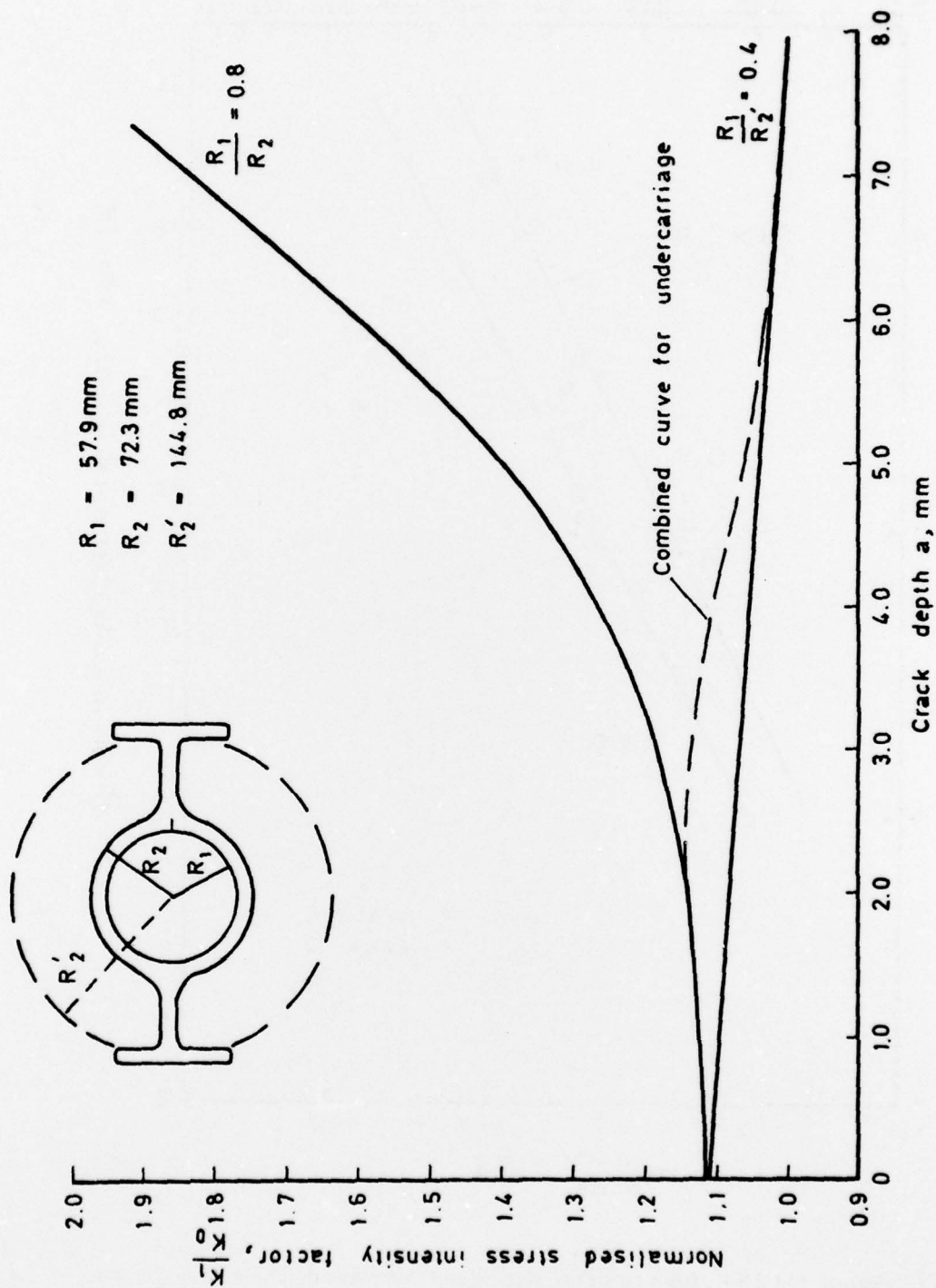
Fig 12 $\frac{K_1}{K_0}$ values (from Fig 10) for a pressurised internal radial edge crack in a tube with $\frac{R_1}{R_2}$ ratios of either 0.4 or 0.8. The $\frac{K_1}{K_0}$ factor for the undercarriage is shown as the combined curve
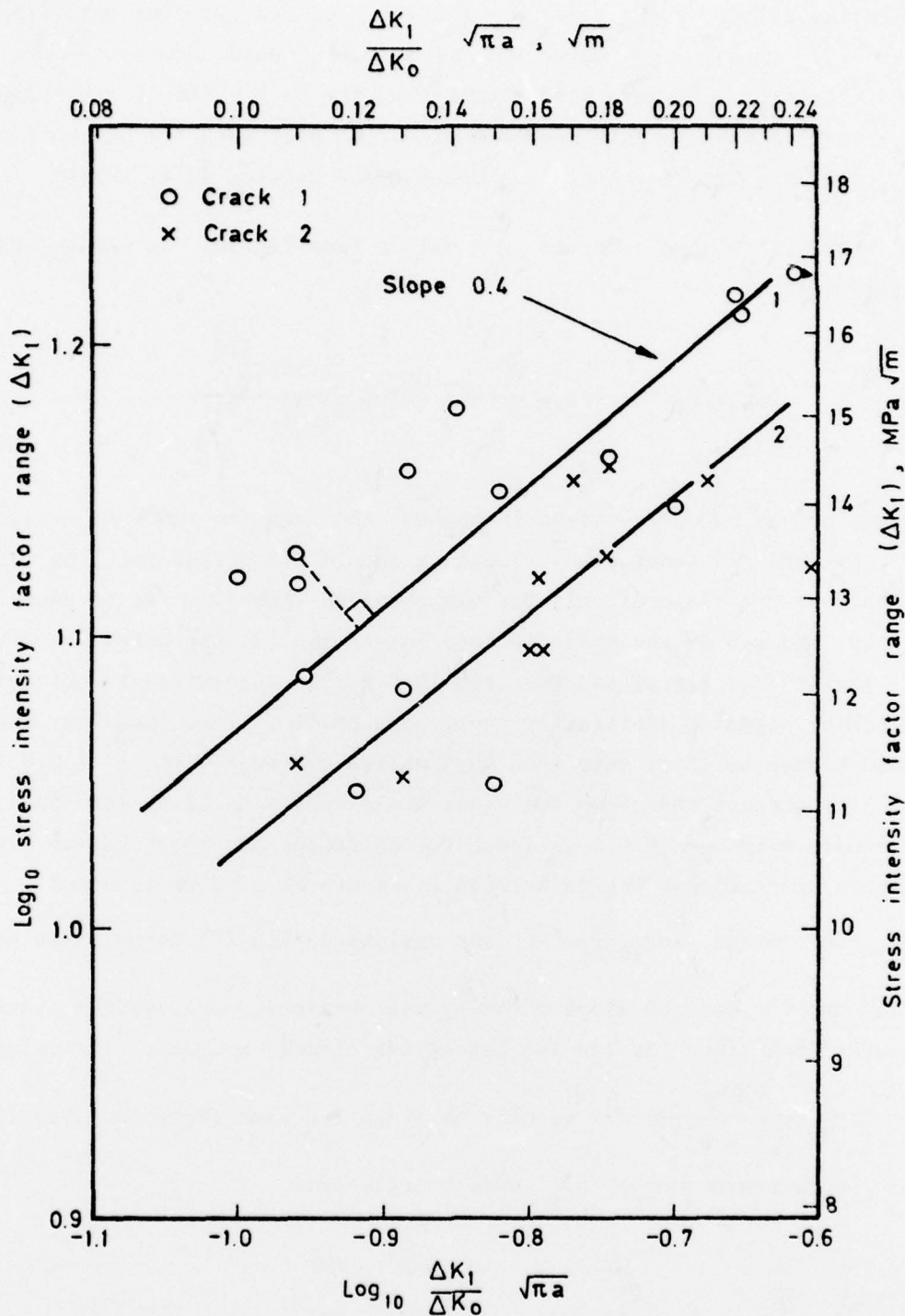
Fig 13

Fig 13   Plot of $\log \Delta K_1$, from striation spacing and Pearson's data[5] versus calculated values of $\log \frac{\Delta K_1}{\Delta K_0} \sqrt{\pi a}$ with $\frac{\Delta K_1}{\Delta K_0}$ taken from the combined curve in Fig 12

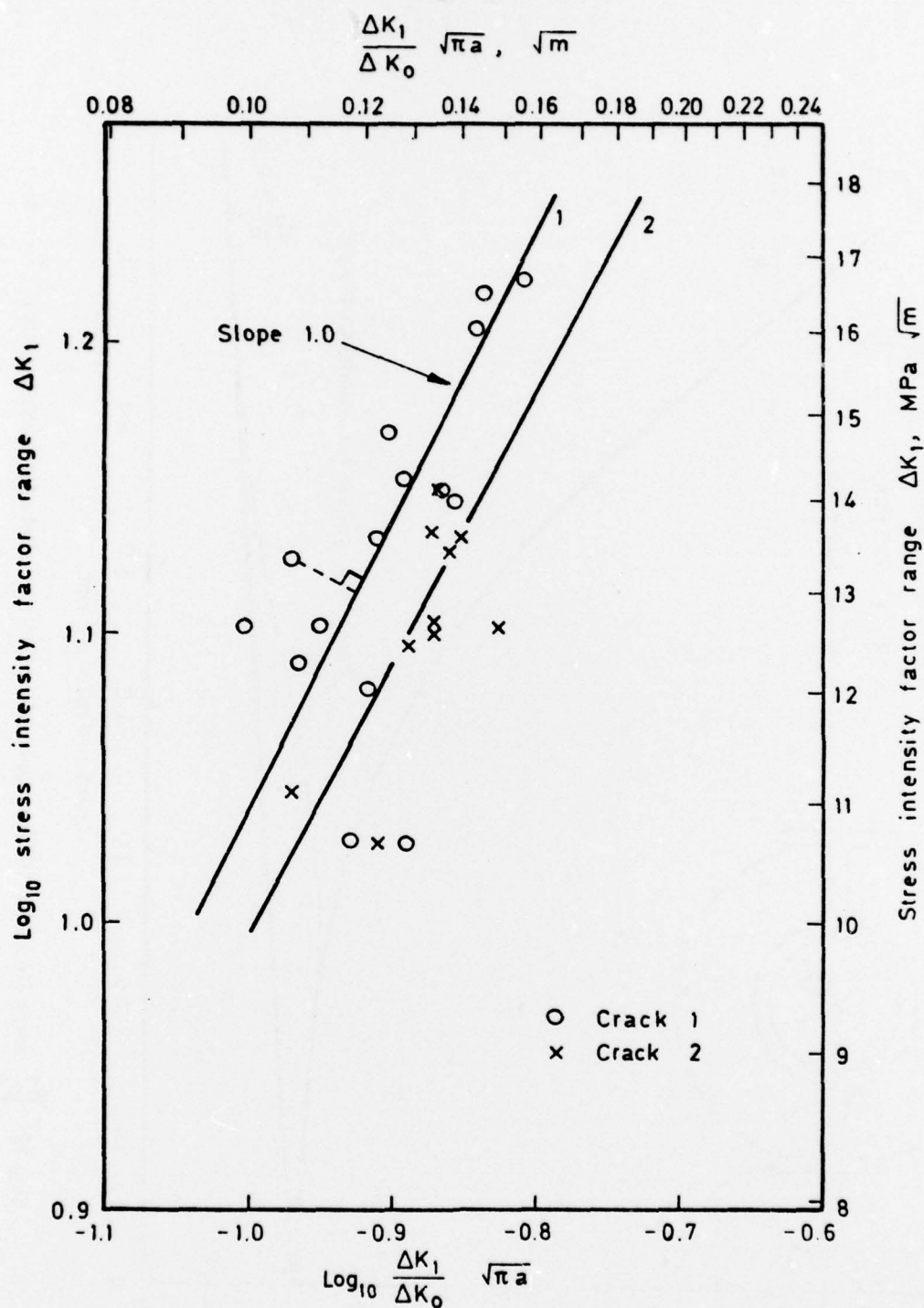## 7   ESTIMATION OF FATIGUE LIFE OF A DEFECT FREE CYLINDER

Engineering Sciences Data sheet[8] 67014 shows the fatigue life of Al-Zn-Mg-Cu alloy (DTD 683) cylinders cyclically pressurised with oil (Fig 14). The ratio of minimum to maximum pressure in the pressure cycle was zero and the value of $\frac{R_1}{R_2}$ was 0.9. The data is presented as fatigue life at different values of the ratio of the maximum elastic shear stress at the bore, q, to the tensile strength of the material, f_t. The value of q was calculated:-

$$q = \Delta p_e \left(\frac{R_2^2}{R_2^2 - R_1^2} \right) \tag{6}$$

and a constant value of 500 MPa was chosen for f_t.

The ratio q/f_t was calculated to be 0.146 and a predicted fatigue life in excess of 2×10^5 B cycles, and possibly more than 10^6 B cycles was read from Fig 14. This is equivalent to at least 1.5×10^4 complete $[(A + B) + 11B]$ pressure sequences. *Thus the defects in the undercarriage reduced the fatigue life by a factor of at least 6.* Alternatively, if the actual life of the defective cylinder of 3.2×10^4 B cycles is compared to Fig 14, the effective q/f_t for the defective cylinder was 0.28 indicating that the fatigue stress concentration factor k_f of the defects was approximately 2.

8   DAMAGE ACCUMULATION

The value of the effective pressure range Δp_e that was obtained was significantly greater than any of the maximum pressures applied during the fatigue loading and an attempt was made to predict the crack growth rates from the actual applied pressures. The B sequence of pressures (Fig 3) was broken down into three components:-

(1)   A ground-air cycle with $\frac{P_{min}}{P_{max}} = 0$ and $\Delta p = 10.6$ MPa.

(2)   A large ground cycle with $\frac{P_{min}}{P_{max}} = 0.4$ and $\Delta p = 6.6$ MPa

(3)   Six small ground cycles with $\frac{P_{min}}{P_{max}} = 0.6$ and $\Delta p = 4.1$ MPa.

Values for ΔK were calculated for increasing crack depths (Table 2) using these Δp values and the combined $\frac{\Delta K_1}{\Delta K_0}$ correction factor for the undercarriage.

20

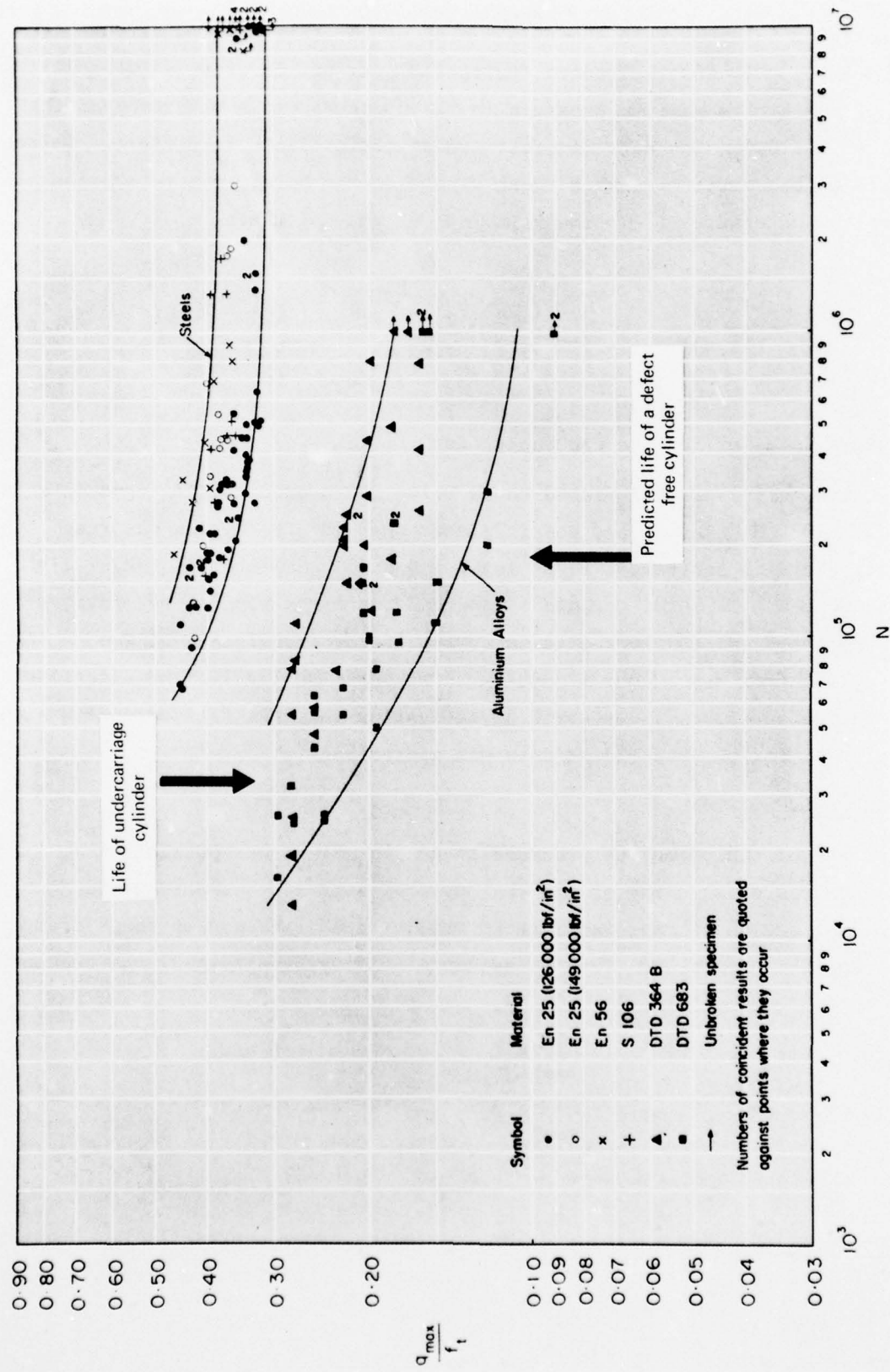Fig 14 Fatigue life (N) of pressurised cylinders as a function of $\dfrac{q}{f_t}$ $\left(\dfrac{\text{maximum elastic shear stress } q}{\text{tensile strength } f_t}\right)$ from Ref 8. Data for DTD 683 is most appropriate to the undercarriage

TR 78078

It can be seen that these individual ΔK cycles were small and prediction of increments of crack growth associated with each ΔK cycle was consequently difficult. Little reliable crack growth data exists for values of ΔK below 5 MPa m$^{\frac{1}{2}}$. The data of Pearson[5] was consequently interpolated to low ΔK values and was compared to the scatter band of data published in a review by Hahn and Simon[9] (Fig 15).

Crack growth rates are thus readily predicted, for each of the components of the B loading sequence, as a function of crack depth and these predicted rates and the accumulated total rate are compared with the measured rates in Fig 16. It is clear that the predicted crack growth rate is less than that observed by a factor of approximately 2. Whilst interactions between high and small loads may explain this discrepancy, it should be remembered that the undercarriage was machined from a forging in DTD 5104 alloy and that the predictions of crack growth rate were based upon laboratory data for DTD 5050 plate, *ie* an alloy of slightly different composition and heat treatment and in a different fabricated form. Moreover, the laboratory data was obtained in dry air and the possibility of a detrimental effect of the hydraulic oil, other than pressurisation of the crack faces, cannot be discounted. A further problem arises from the complicated geometry of the undercarriage and the curved crack front. It is interesting to note that the six small ground cycles were very damaging.

9   DISCUSSION

Fatigue substantiation tests of aircraft components frequently raise the question "Was the fatigue life of the component consistent with the fatigue properties of the basic material?" In simple cases of defect-free material and uniform fatigue loadings, fatigue lives may be predicted from laboratory data. This Report analyses the case of a complicated programmed loading sequence applied to an undercarriage of complex shape with further problems associated with the presence of material defects and hydraulic oil. The analytical technique based upon the measurement of fatigue striation spacings enabled the number of fatigue loading sequences, taken to grow the cracks from initiation at defects to final failure, to be determined and since this was a large proportion of the applied fatigue life (>67%) it can be concluded that early initiation of the fatigue cracks at the metallurgical defects reduced the total fatigue life by a considerable amount. This amount was quantified by the introduction of a concept of effective pressure, a simple sinusoidal fluctuation in pressure, equivalent in its effects on the rate of fatigue crack growth, to the whole B sequence of pressure cycles. This enabled the fatigue life of a defect free cylinder to be predicted,
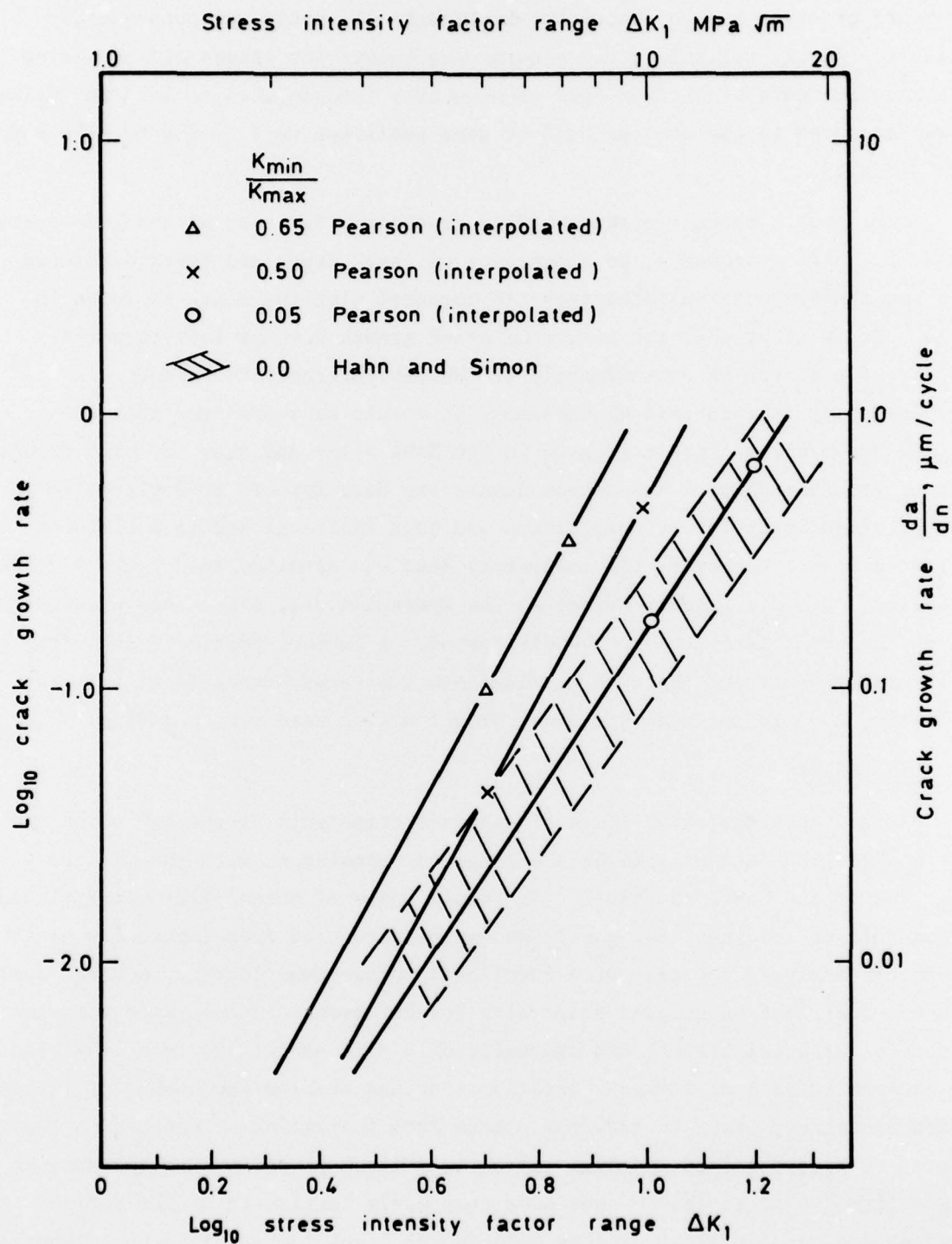
Fig 15

Fig 15   Fatigue crack growth rates for DTD 5050 interpolated, from the data
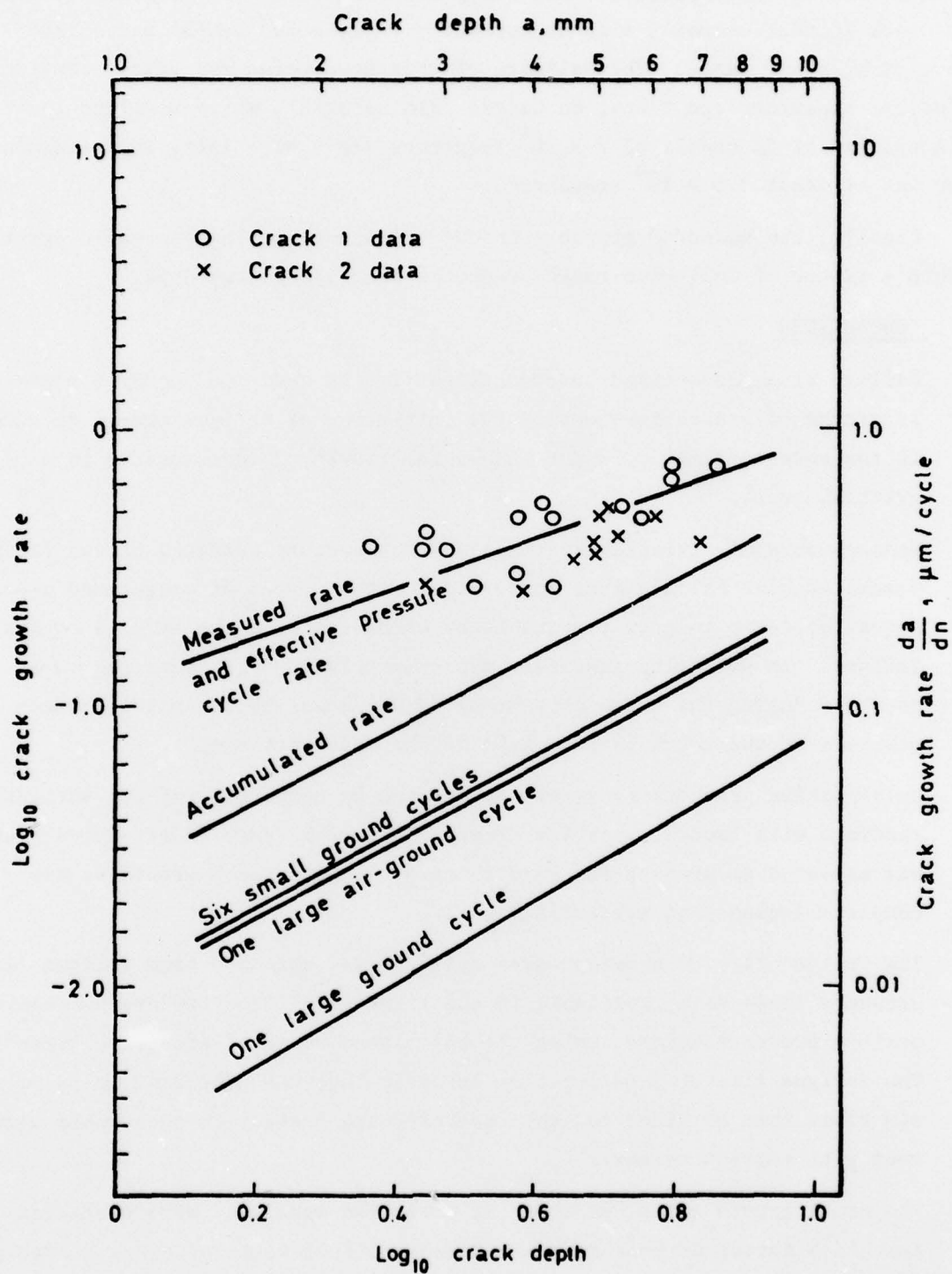of Pearson, for low values of ΔK_1

Fig 16

Fig 16 Measured fatigue crack growth rates and growth rates predicted by the addition of increments of growth for each of the individual pressure cycles (*cf* Fig 3)

24

provided that the assumption was made that the effects of the programme loading upon crack initiation would also be correctly represented by the use of the effective pressure range. The validity of this assumption was partly confirmed by further undercarriage tests, on defect free material, which resulted in fatigue lives of in excess of 2×10^4 sequences [(A + B) + 11B], the predicted value was at least 1.5×10^4 sequences.

Finally, the measured growth rates were found to be in reasonable agreement (within a factor of 2-3) with rates predicted from laboratory data.

10   CONCLUSIONS

(1)   Failure of a pressurised undercarriage fitting occurred, under a repeated programme of pressurisations, by the initiation of fatigue cracks at defects in the undercarriage cylinder and by the growth of these cracks to a critical depth.

(2)   Measurements of striation spacings on the fracture surfaces of two fatigue cracks enabled calculations to be made of the number of programmed pressure sequences taken to grow the cracks by extension from the defects to final failure. It was calculated that approximately 2000 pressure sequences occurred during the crack growth period which was approximately three-quarters of the total fatigue life of the undercarriage.

(3)   An effective pressure range was calculated by comparison of the striation spacings with laboratory crack growth data. The range in effective pressure was selected to produce the same rates of fatigue crack growth as one complete sequence of pressurisations.

(4)   The fatigue life of a defect free cylinder was obtained from fatigue life-pressure range data, available in the literature for cylinders undergoing uniform pressurisations, using the calculated range of effective pressure. The fatigue life of a defect free undercarriage was predicted to be at least six times that obtained for the undercarriage tested, in reasonable agreement with subsequent tests.

(5)   The crack growth rates, measured as striation spacings, were predicted (within a factor of 2-3) by the addition of increments of crack growth predicted for the individual pressure cycles of the programme sequence.

078

Table 1

Striation spacings, stress intensity factor ranges predicted from Pearson's data, $\frac{\Delta K_1}{\Delta K_0}$ correction factors taken from Bowie and Freese and calculated values of $\frac{\Delta K_1}{\Delta K_0} \sqrt{\pi a}$.

	Crack depth mm	Striation spacing μm/cycle	ΔK_1 MPa $\sqrt{m}$	$\frac{\Delta K_1}{\Delta K_0}$	$\frac{\Delta K_1}{\Delta K_0} \sqrt{\pi a}$ $\sqrt{m}$
Crack 1	2.32	0.39	12.7	1.13	0.096
	2.79	0.33	12.3	1.15	0.108
	2.83	0.43	13.3	1.15	0.108
	3.01	0.38	12.7	1.14	0.111
	3.30	0.27	10.7	1.13	0.116
	3.81	0.31	12.0	1.11	0.121
	3.82	0.50	13.6	1.11	0.122
	4.10	0.56	14.8	1.10	0.125
	4.24	0.27	10.7	1.09	0.126
	4.25	0.49	14.1	1.09	0.126
	5.37	0.52	14.2	1.05	0.136
	5.73	0.48	14.0	1.03	0.138
	6.15	0.65	16.0	1.02	0.142
	6.18	0.70	16.5	1.02	0.143
	7.31	0.73	16.7	1.01	0.153
Crack 2	2.78	0.28	11.1	1.14	0.107
	3.85	0.27	10.7	1.11	0.122
	4.58	0.35	12.5	1.08	0.128
	4.85	0.36	12.6	1.07	0.131
	4.86	0.38	12.7	1.07	0.131
	5.00	0.50	13.6	1.06	0.140
	5.15	0.52	14.1	1.06	0.134
	5.27	0.44	13.4	1.05	0.135
	5.90	0.50	13.6	1.03	0.132
	6.90	0.39	12.7	1.01	0.149

Table 2

Crack growth rates, predicted from Pearson's data, for damage accumulation calculations.

	Crack depth mm	$\dfrac{\Delta K_1}{\Delta K_0}$	ΔK_1 MPa $\sqrt{m}$	Predicted growth rate μm/cycle
Air-ground cycle	1	1.10	3.63	0.008
	2	1.14	5.32	0.024
	3	1.15	6.57	0.048
$\dfrac{K_{min}}{K_{max}} = 0.0$	4	1.11	7.33	0.068
	5	1.05	7.75	0.076
$\Delta p = 10.56$ MPa	6	1.03	8.33	0.096
	7	1.01	8.82	0.115
	8	1.00	9.34	0.138
Large ground cycle	1	1.10	2.17	0.003
	2	1.14	3.17	0.008
	3	1.15	3.92	0.018
$\dfrac{K_{min}}{K_{max}} = 0.4$	4	1.11	4.37	0.023
	5	1.05	4.62	0.029
	6	1.03	4.97	0.040
$\Delta p = 6.56$ MPa	7	1.01	5.26	0.050
	8	1.00	5.57	0.059
Small ground cycle	1	1.10	1.38	<0.001
	2	1.14	2.00	0.004
	3	1.15	2.50	0.007
$\dfrac{K_{min}}{K_{max}} = 0.57$	4	1.11	2.79	0.011
	5	1.05	2.95	0.014
	6	1.03	3.17	0.020
$\Delta p = 4.10$ MPa	7	1.01	3.35	0.023
	8	1.00	3.55	0.030

REFERENCES

No.	Author	Title, etc
1	P.J.E. Forsyth D.A. Ryder	Fatigue fracture. Aircraft Engineering, 32, p 96 (1960)
2	C.J. Peel	An analysis of a test fatigue failure by fractography and fracture mechanics. RAE Technical Report 72034 (1972)
3	D. Cruickshanks-Boyd	A comparison of fatigue crack growth rates as determined by striation measurements and by observations of crack length on the specimen surface during the test. RAE Technical Report 76012 (1976)
4	S. Pearson	Fatigue crack initiation and propagation in half inch thick specimens of an aluminium alloy. RAE Technical Report 71109 (1971)
5	S. Pearson	The effect of mean stress on the fatigue crack propagation in half inch thick specimens of aluminium alloys of high and low fracture toughness. RAE Technical Report 68297 (1968)
6	D.P. Rooke D.J. Cartwright	Compendium of stress intensity factors. HMSO London (1976)
7	O.L. Bowie C.E. Freese	Eng. Frac. Mech., 4, p 315 (1972)
8	Royal Aeronautical Society Institute of Mechanical Engineering	Fatigue strength of thick cylinders under internal pressure. Engineering Sciences Data No.67014, Royal Aeronautical Society (1967)
9	G.T. Hahn R. Simon	A review of fatigue crack growth in high strength Al alloys and relevant metallurgical factors. Eng. Frac. Mech., 5, (3), p 523 (1973)

REPORT DOCUMENTATION PAGE

Overall security classification of this page

UNLIMITED

As far as possible this page should contain only unclassified information. If it is necessary to enter classified information, the box above must be marked to indicate the classification, e.g. Restricted, Confidential or Secret.

1. DRIC Reference (to be added by DRIC)	2. Originator's Reference RAE TR 78078	3. Agency Reference N/A	4. Report Security Classification/Marking UNLIMITED

5. DRIC Code for Originator 850100	6. Originator (Corporate Author) Name and Location Royal Aircraft Establishment, Farnborough, Hants, UK
5a. Sponsoring Agency's Code N/A	6a. Sponsoring Agency (Contract Authority) Name and Location N/A

7. Title An analysis of a programmed load fatigue failure

7a. (For Translations) Title in Foreign Language

7b. (For Conference Papers) Title, Place and Date of Conference

N/A

8. Author 1. Surname, Initials Peel, C.J.	9a. Author 2	9b. Authors 3, 4	10. Date July 1978	Pages 27	Refs. 9
11. Contract Number N/A	12. Period N/A	13. Project N/A	14. Other Reference Nos. Mat 358		

15. Distribution statement
    (a) Controlled by — ~~AD/XR Materials via DRIC~~

    (b) Special limitations (if any) — None

16. Descriptors (Keywords)   (Descriptors marked * are selected from TEST)
    Fatigue.   Fatigue striations.   Fracture mechanics.

17. Abstract

    Premature failure of an undercarriage fitting occurred during a fatigue test, in which the cylindrical barrel of the undercarriage was internally pressurised in a programmed sequence of pressures representing landing and taxying loads. Failure occurred by the initiation of fatigue cracks at defects in the undercarriage forging and by their growth to a critical depth. Measurement of the spacings of fatigue striations, on the surfaces of two cracks, enabled calculations to be made of the number of pressure sequences taken to grow the cracks from initiation to final failure.

    An effective pressure range was calculated by comparison of the fatigue striation spacings with laboratory crack growth data. It was assumed that one cycle of the effective pressure range would produce the same rate of crack growth as an entire sequence of pressurisations. The effective pressure range was used to predict the fatigue life of a defect free undercarriage by reference to the pressure-fatigue life data found in the literature. It was found, by this means, that the metallurgical defects had reduced the life of the cylinder by a factor of at least 6 and that they had an effective stress concentration factor in fatigue of approximately 2.

RAE Form A143